Original Paper

Cellular Physiology and Biochemistry

Cell Physiol Biochem 2011;28:911-922

Accepted: August 26, 2011

Depletion of 14-3-3 Protein Exacerbates Cardiac Oxidative Stress, Inflammation and Remodeling Process via Modulation of MAPK/NF-κB Signaling Pathways after Streptozotocin-induced Diabetes Mellitus

Rajarajan A. Thandavarayan[1,2], Vijayasree V. Giridharan[2], Flori R. Sari[1], Somasundaram Arumugam[1], Punniyakoti T. Veeraveedu[1], Ganesh N. Pandian[3], Suresh S. Palaniyandi[4], Meilei Ma[1], Kenji Suzuki[5], Narasimman Gurusamy[6] and Kenichi Watanabe[1]

[1]Department of Clinical Pharmacology, Niigata University of Pharmacy and Applied Life Sciences, Niigata city, [2]Department of Functional and Analytical Food sciences, Niigata University of Pharmacy and Applied Life Sciences, Niigata city, [3]Institute for Integrated Cell–Material Sciences, Kyoto University, Yoshida-ushinomiyacho, Kyoto, [4]Department of Chemical and System Biology, Stanford University School of Medicine, Stanford, CA, [5] Department of Gastroenterology and Hepatology, Niigata University Graduate School of Medical and Dental Sciences, Niigata, [6]Department of Anesthesiology and Medicine, Brigham and Women's Hospital, Harvard Medical School, Boston, MA

Key Words

Diabetic cardiomyopathy • 14-3-3 protein • Oxidative stress • p38 MAPK • Inflammation

Abstract

Diabetic cardiomyopathy is associated with increased oxidative stress and inflammation. Mammalian 14-3-3 proteins are dimeric phosphoserine-binding proteins that participate in signal transduction and regulate several aspects of cellular biochemistry. The aim of the study presented here was to clarify the role of 14-3-3 protein in the mitogen activated protein kinase (MAPK) and nuclear factor-kB (NF-κB) signaling pathway after experimental diabetes by using transgenic mice with cardiac-specific expression of a dominant-negative 14-3-3 protein mutant (DN 14-3-3). Significant p-p38 MAPK activation in DN 14-3-3 mice compared to wild type mice (WT) after diabetes induction and with a corresponding up regulation of its downstream effectors, p-MAPK activated protein kinase 2 (MAPKAPK-2). Marked increases in cardiac hypertrophy, fibrosis and inflammation were observed with a corresponding up-regulation of atrial natriuretic peptide, osteopontin, connective tissue growth factor, tumor necrosis factor α, interleukin (IL)-1β, IL-6 and cellular adhesion molecules. Moreover, reactive oxygen species, left ventricular expression of NADPH oxidase subunits, p22 phox, p67 phox, and Nox4, and lipid peroxidation levels were significantly increased in diabetic DN 14-3-3mice compared to diabetic WT mice. Furthermore, myocardial NF-κB activation, inhibitor of kappa B-α degradation and mRNA expression of proinflammatory

KARGER

Fax +41 61 306 12 34
E-Mail karger@karger.ch
www.karger.com

1015-8987/11/0285-0911$38.00/0

Accessible online at:
www.karger.com/cpb

Professor Kenichi Watanabe
Department of Clinical Pharmacology, Faculty of Pharmaceutical Sciences
Niigata University of Pharmacy and Applied Life Sciences
265-1 Higashijima Akiha-ku, Niigata city, 956-8603 (Japan)
Tel. +81-250-25-5267, Fax +81-250-25-5021, E-Mail watanabe@nupals.ac.jp

cytokines were significantly increased in DN 14-3-3 mice compared to WT mice after diabetes induction. In conclusion, our data suggests that depletion of 14-3-3 protein induces cardiac oxidative stress, inflammation and remodeling after experimental diabetes induction mediated through p38 MAPK, MAPKAPK-2 and NF-κB signaling.

Introduction

Cardiovascular complications, including diabetic cardiomyopathy, are the major cause of fatalities in diabetes. Diabetic cardiomyopathy is a distinct entity independent of coronary artery disease [1, 2] despite earlier beliefs common in the diabetic population [3]. Experimental models of diabetes mellitus, such as streptozotocin (STZ)-induced type 1 diabetes mellitus, imitate the structural and cellular abnormalities of diabetic cardiomyopathy [4]. These abnormalities include, among others, cardiac fibrosis [5] and cardiac inflammation, which lead to left ventricular (LV) dysfunction, mediated mainly by the diabetic milieu (e.g. high glucose levels, oxidative stress, angiotensin II) [2, 4, 6]. Cardiac inflammation, not only in diabetic cardiomyopathy, but also in most kinds of heart failure, is accompanied by elevated cardiac protein levels of cytokines, such as tumor necrosis factor α (TNF- α), interleukin 1 β (IL-1 β), IL6, and transforming growth factor β1(TGF- β1). These elevated cytokine levels are not only present in the cardiac tissue of animal models [7], but also in the serum of diabetic patients [8]. Nuclear Factor-κB (NF-κB) is a key transcription factor that regulates inflammatory processes [9]. Given that increased levels of cytokines correlate with cardiac failure in humans [10], cardiac inflammation might be important in diabetic patients, too.

14-3-3 protein belongs to a class of highly conserved proteins involved in regulating apoptosis, adhesion, cellular proliferation, differentiation, survival, and signal transduction pathways [11]. Apoptosis signal-regulating kinase 1 (Ask-1), a mitogen activated protein kinase kinase kinase, is involved in biological responses such as apoptosis, inflammation, differentiation and survival in different cell types. Activated Ask1 relays signals to c-jun NH_2 kinase (JNK) and p38 mitogen activated protein kinase (MAPK) [12, 13]. Recent studies have indicated that NF-κB may play important roles in cardiac hypertrophy and remodeling besides promoting inflammation [9]. Hence the specific role of MAPK and NF-κB in the development of diabetic cardiomyopathy should be examined. We have recently reported that transgenic mice with cardiac specific-expression of a dominant-negative mutant of 14-3-3η protein (DN 14-3-3η) exhibit that development of diabetic cardiomyopathy is accelerated after disruption of 14-3-3 protein function, in part through enhancement of the Ask1 signaling pathway [14]. However, the specific role of 14-3-3 protein-MAPK-NF-κB signaling pathway in the development of diabetic cardiomyopathy has been not directly demonstrated. Based on our previous findings, we postulated that DN 14-3-3η mice could provide a model for the investigation of MAPK-NF-κB signaling in the STZ -induced cardiac remodeling process.

We here demonstrate that 14-3-3 protein acts as an endogenous cardioprotector and limits the development of diabetic cardiomyopathy by limiting oxidative stress, myocardial inflammation, hypertrophy and fibrosis, via inhibition of p38 MAPK/MAPKAPK-2/NF-κB signaling after induction of experimental diabetes.

Materials and Methods

Generation of DN 14-3-3η transgenic mice

Transgenic DN 14-3-3η mice were generated as described previously [15]. Briefly, the coding region of human DN (R56A and R60A) 14-3-3η cDNA with a 5′-Myc-1 epitope tag was subcloned into a vector containing the α-myosin heavy chain promoter and an SV40 polyadenylation site. Linearized DNA was injected into the pronuclei of one-cell C57BL/6 XSJL embryos at the Neuroscience Transgenic Facility at Washington University School of Medicine. Progeny were backcrossed into the C57BL/6 genetic background and were analyzed by polymerase chain reaction to detect transgene integration using mouse-tail DNA as template. Age matched C57BL/6 JAX mice (obtained from Charles River Japan Inc., Kanagawa, Japan) were used as wild type (WT) controls. Mice were maintained with free access to water and chow throughout the period of study, and animals were treated in accordance with the Guidelines for Animal Experimentation of our institute. All animals were handled according to the approved protocols and animal welfare regulations of the Institutional Review Board at Niigata University of Pharmacy and Applied Life Sciences.

Diabetes induction

Diabetes was induced by a single intraperitoneal injection of STZ (150 mg/kg body wt; Sigma-Aldrich Inc., St.Louis, USA) dissolved in vehicle (20 mM sodium citrate buffer pH 4.5) to 10-12 week old male WT and DN 14-3-3η mice. As a control, vehicle (100 μl of citrate buffer) was injected in age matched DN 14-3-3η and WT mice. Random blood glucose measurements

were performed using Medi-safe chips (Terumo Inc., Tokyo, Japan) at 7 day interval. Animals were considered to be diabetic if they had a random blood glucose levels higher than 300 mg/dl. All other physiological, anatomic and biochemical studies performed on animals at 28 days after STZ injection.

Protein analysis

Cytoplasmic and nuclear fraction protein lysate were prepared from heart tissue as described previously [16, 17]. The total protein concentration in samples was measured by the bicinchoninic acid method. For Western blotting experiments, 100 μg of total protein was loaded and proteins were separated by SDS-PAGE (200 V for 40 min) and electrophoretically transferred to nitrocellulose filters (semi-dry transfer at 10 V for 30 min). Filters were blocked with 5% non-fat dry milk in Tris buffered saline (20mM Tris, pH 7.6, 137 mM Nacl) with 0.1% Tween 20, washed, and then incubated with primary antibody. Primary antibodies employed included: rabbit polyclonal, phosho-p38 MAPK, phospho-mitogen activated protein kinase-activated protein kinase 2 (p-MAPKAPK-2) a downstream effector of p38 MAPK, intercellular adhesion molecule-1 (ICAM-1), inhibitor of kappa Bα(IκBα) and rabbit monoclonal NF-κB (Cell Signaling Technology Inc., MA, USA), rabbit polyclonal atrial natriuretic peptide (ANP), connective tissue growth factor (CTGF), vascular cell adhesion molecule-1 (VCAM-1), p67-phox and p22-phox, mouse polyclonal osteopontin, goat polyclonal Nox4, TNF-α, IL-1β and glyceraldehyde-3-phosphate dehydrogenase (GAPDH) (Santa Cruz Biotechnology Inc., CA, USA). After incubation with the primary antibody, the bound antibody was visualized with horseradish peroxidase-coupled secondary antibodies (Santa Cruz Biotechnology) and chemiluminescence developing agents (Amersham Biosciences, Buckinghamshire, UK). The level of expression of each protein in control WT mice was taken as one arbitrary unit (AU). For western blotting analysis, all primary antibodies were used at a dilution of 1:1000 and secondary antibodies were used at a dilution of 1:5000. Films were scanned and band densities were quantified by densitometric analysis using Scion image software (Epson GT-X700; Tokyo, Japan).

Cytochrome c reduction assay

NADPH dependent superoxide production was examined using superoxide dismutase (SOD)-inhibitable cytochrome *c* reduction [18]. Total protein from myocardial tissue (final concentration 1 mg/ml) was distributed in 96-well plates (final volume 200 μl/well). Cytochrome *c* (500 μmol/L) and NADPH (100 μmol/L) were added in the presence or absence of SOD (200 U/ml) and incubated at room temperature for 30 min. Cytochrome *c* reduction was measured by reading absorbance at 550-nm wavelength on a microplate reader. Superoxide production was calculated from the difference between absorbance with and without SOD and extinction coefficient for change of ferricytochrome c to ferrocytochrome c, i.e., 21.0 mmol L^{-1} cm^{-1}.

Measurement of Reactive oxygen species (ROS)

ROS levels were measured using the fluorescence indicator 2',7'-dichlorofluorescein (DCFH), as previously described [19]. When DCFH is added to the tissue homogenate, ROS in the homogenate will lead to the oxidation of DCFH, producing the fluorescent product dichlorofluorescein. In our experiment, 5 μM DCFH was incubated with 100 μL containing 100 μg LV cytosolic proteins, and fluorescence was recorded following 1 h incubation using a microplate spectrofluorometer (Fluoroskan Ascent CF, Labsystems, MA, USA) at an excitation wavelength of 485 nm and an emission wavelength of 530 nm.

Thiobarbituric acid reactive substances (TBARS) assay

Levels of TBARS were measured in homogenates of heart tissues using a commercial kit (Oxitek, ZeptoMetrix Corporation, Buffalo, NY, U.S.A.). Hearts that had been used in the functional experiments were homogenized in normal saline and 100 μl of protein suspension were combined with 2.5 ml of thiobarbituric acid from the assay kit, incubated for 1 h at 95°C, cooled to room temperature and centrifuged at 3000 rpm for 15 min. The supernatant was analyzed by sprectrophotometer (532 nm) for the reaction product between thiobarbituric acid and malondialdehyde (MDA), which latter results from lipid peroxidation. TBARS levels were expressed as nmol MDA per milligram protein. The standard curve comprised 0 –100 nmol/ml MDA.

Myocardial cell size measurement

Paraffin embedded LV tissue sections stained with hematoxylin and eosin (H-E), were used for measuring cell size. Short axis diameter of cardiac myocyte was measured for 10 myocytes selected per field (about 50 fields were selected per section) at 400-fold magnification by light microscopy (CIA-102, Olympus, Tokyo, Japan). Each average value was obtained based on the data from 10 myocytes and was used as an independent sampling data [20, 21].

Measurement of myocardial fibrosis

The area of myocardial fibrosis in LV tissue sections stained with Azan-Mallory was quantified using a color image analyzer (CIA-102, Olympus, Tokyo, Japan) and measuring the blue fibrotic areas as opposed to the red myocardium at 200x magnification. The results were presented as the ratio of the fibrotic area to the whole area of the myocardium [20]. Digital photographs were taken using the color image analyzer (CAI-102; Olympus, Tokyo, Japan).

In situ detection of superoxide production in hearts

To evaluate in situ superoxide production from hearts, unfixed frozen cross sections of the specimens were stained with dihydroethidium (DHE; Molecular Probe, OR) according to the previously validated method [22-25]. In the presence of superoxide, DHE is converted to the fluorescent molecule ethidium, which can then label nuclei by intercalating with DNA. Briefly, the unfixed frozen tissues were cut into 10-μm-thick

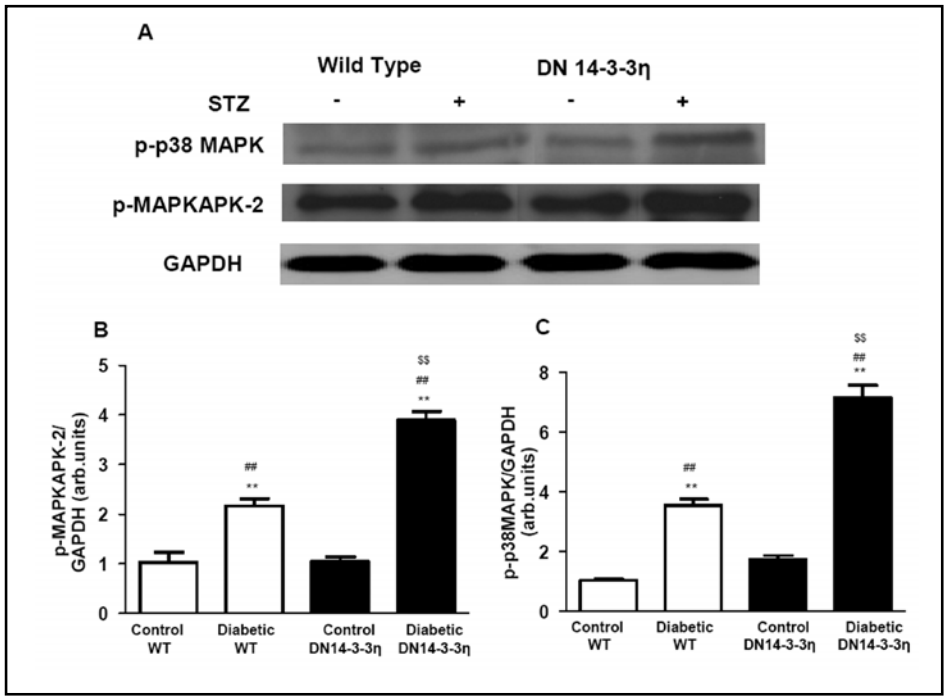

Fig. 1. Representative western immunoblots and densitometry analysis using Scion image software for p-p38 MAPK (A and C) and p-MAPKAPK-2 (A and B) levels in control (-) and 28 days after STZ injection (+). Blots were normalized to GAPDH. White and black bars represent WT and DN 14-3-3η mice, respectively. Each bar represents means ± S.E. (n=4 to 5). $^{**}P < 0.01$ vs. control WT mice; $^{\#\#}P < 0.01$ vs. control DN 14-3-3η mice; $^{\$\$}P < 0.01$ vs. diabetic WT mice on the same day.

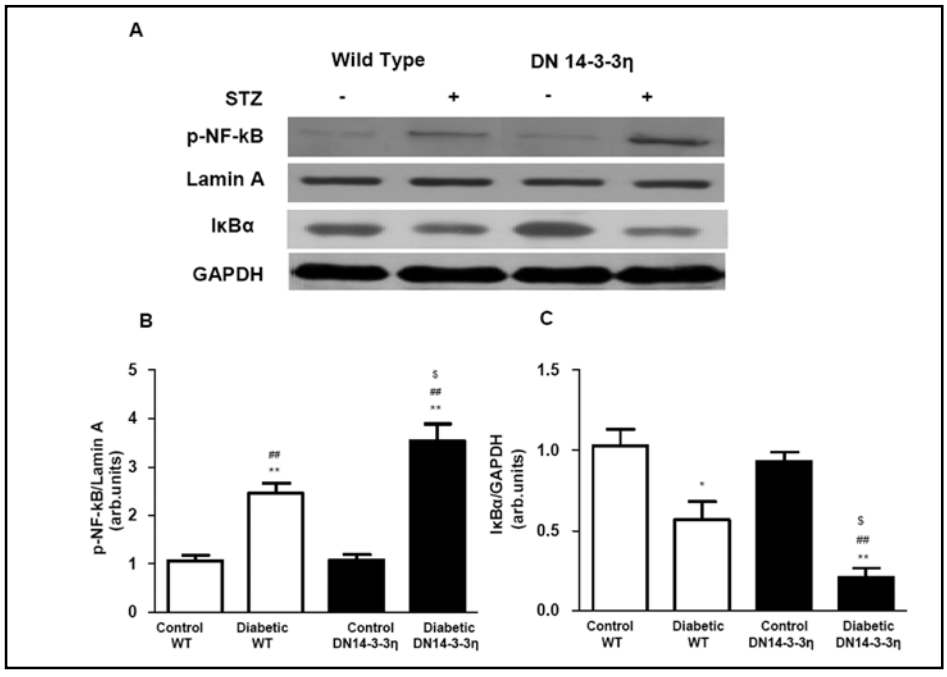

Fig. 2. Representative western immunoblots and densitometry analysis using Scion image software for p-NF-κB (A and B) and IκBα (A and C) levels in control (-) and 28 days after STZ injection (+). Blots were normalized to Lamin A and GAPDH respectively. White and black bars represent WT and DN 14-3-3η mice, respectively. Each bar represents means + S.E. (n=4 to 5). $^{*}P < 0.05$ vs. control WT mice; $^{**}P < 0.01$ vs. control WT mice; $^{\#\#}P < 0.01$ vs. control DN 14-3-3η mice; $^{\$}P < 0.05$ vs. diabetic WT mice on the same day.

sections and incubated with 10 μM DHE at 37°C for 30 min in a light-protected humidified chamber. Fluorescence images were obtained using a fluorescence microscope equipped with a rhodamine filter.

RNA Extraction

Heart tissues were preserved by immersion in RNAlater (Ambion Inc., Austin, TX) immediately after sampling. The extraction of total RNA was performed after homogenization by using Ultra TurraxT8 (IKA Labortechinik, Staufen, Germany) in TRIzol reagent (invitrogen Corp., CA) according to the standard protocol. Synthesis of cDNA was performed by reverse transcription using total RNA (2 μg) as a template (Super Script II; Invitrogen Corporation, Carlsbad, CA).

Gene expression analysis by real time RT-PCR

Gene expression analysis was performed by real time reverse transcription polymerase chain reaction (RT-PCR) (Smart cycler; Cepheid, Sunnyvale, CA) using cDNA synthesized from the heart samples. Primer used in this study as follows: IL-1β, IL-6, TNF-α and GAPDH. Real time RT-PCR by monitoring with TaqMan probe (TaqMan Gene

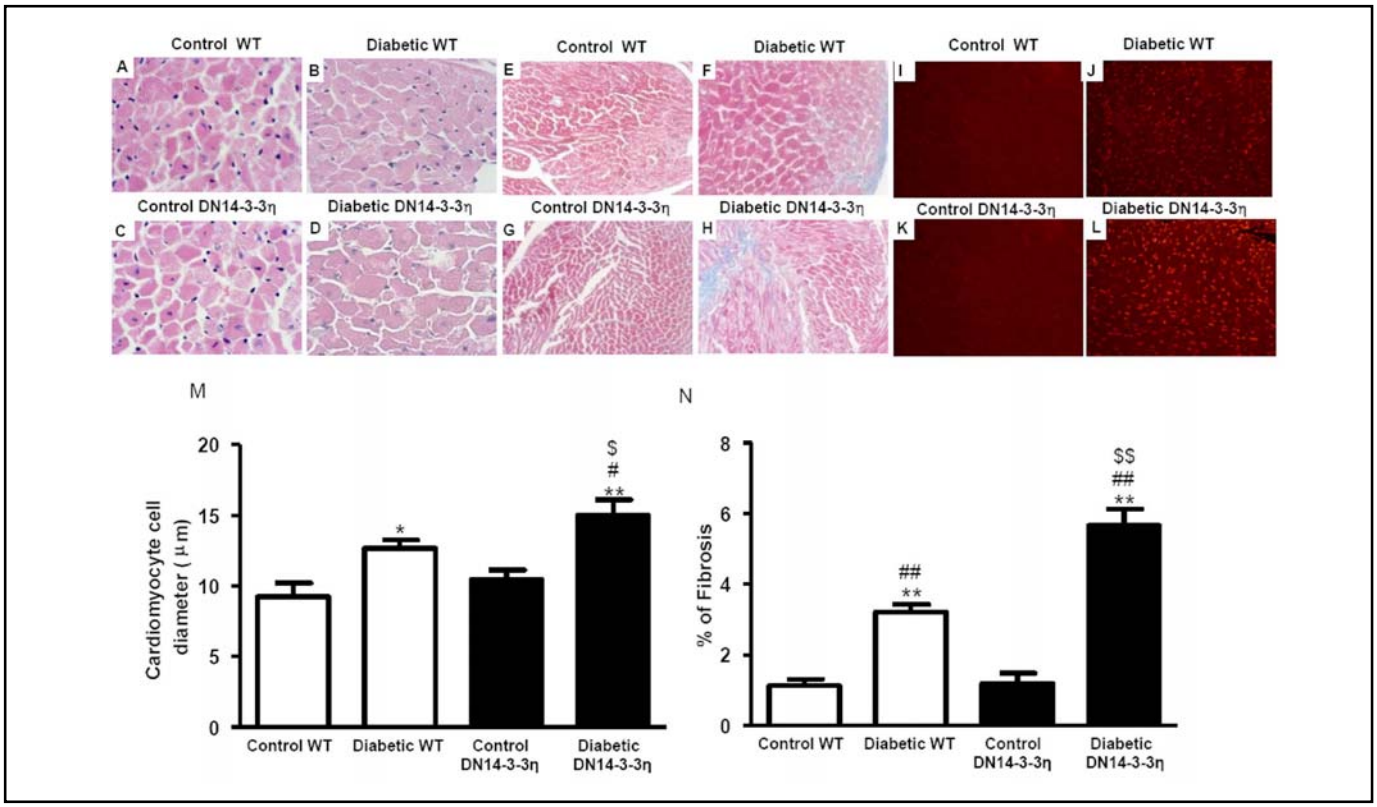

Fig. 3. 14-3-3 protein protects against cardiac remodeling after diabetes. (A-D) Myocardial tissue sections stained with H-E showing cross-sectional area of cardiomyocytes in control and diabetic WT mice (A and B, respectively), as well as control and diabetic DN 14-3-3η mice (C and D, respectively) at 400x magnification. (E-H) Azan Mallory staining showing interstitial fibrosis in control and diabetic WT mice (E and F, respectively), as well as control and diabetic DN 14-3-3η mice (G and H, respectively) at 200x magnification; Note the extra cellular matrix content (blue color) and disarray in diabetic DN 14-3-3η mice. (I-L) *In situ* superoxide production (bright area) using dihydroethidium (DHE) staining in control and diabetic WT mice (I and J, respectively), as well as control and diabetic DN 14-3-3η mice (K and L, respectively) at 200x magnification. (M and N) Bar graph shows quantitative analysis of cardiomyocyte cell diameter (M) and interstitial fibrosis (N), in control and diabetic myocardium respectively. White and black bars represent WT and DN 14-3-3η mice, respectively. Each bar represents means ± S.E. (n=4 to 5). $^{*}P < 0.05$ vs. control WT mice; $^{**}P < 0.01$ vs. control WT mice; $^{\#}P < 0.05$ vs. control DN 14-3-3η mice; $^{\#\#}P < 0.01$ vs. control DN 14-3-3η mice; $^{\$}P < 0.05$ vs. diabetic WT mice on the same day; $^{\$\$}P < 0.01$ vs. diabetic WT mice on the same day.

expression assays; Applied Biosystems, Foster City, CA) was performed according to the following protocol: 600 seconds at 95 ºC, followed by thermal cycles of 15 seconds at 95 ºC, and 60 seconds at 60 ºC for extension. Relative standard curves representing several 10 fold dilutions (1:10:100:1000:10,000:100,000) of cDNA from heart tissue samples were used for linear regression analysis of other samples. Results were normalized to GAPDH mRNA as an internal control and are thus shown as relative mRNA levels.

Statistical analysis

Data were presented as means ± standard error (S.E.) and were analyzed using one-way analysis of variance (ANOVA) followed by Tukey or Bonferroni methods for post hoc analysis and two-tailed t-test when appropriate. A value of $P<0.05$ was considered statistically significant. For statistical analysis GraphPad Prism 5 software (San Diego, CA, U.S.A.) was used.

Results

Phospho-p38 MAPK and phospho-MAPKAPK-2 expression

LV expression of phospho-p38 MAPK and phospho-MAPKAPK-2 were significantly increased in WT and DN 14-3-3η mice at 28 days after STZ injection when compared to respective control mice (Fig. 1A-C). However DN 14-3-3η mice had significantly ($P < 0.01$) increased p38 MAPK and MAPKAPK-2 activation when compared to WT mice (Fig. 1A-C).

NF-κB activation and IκBα degradation

A higher expression level of p-NF-κB corresponded to significant IκBα degradation in DN 14-3-3η and WT mice at 28 days after diabetes induction relative to

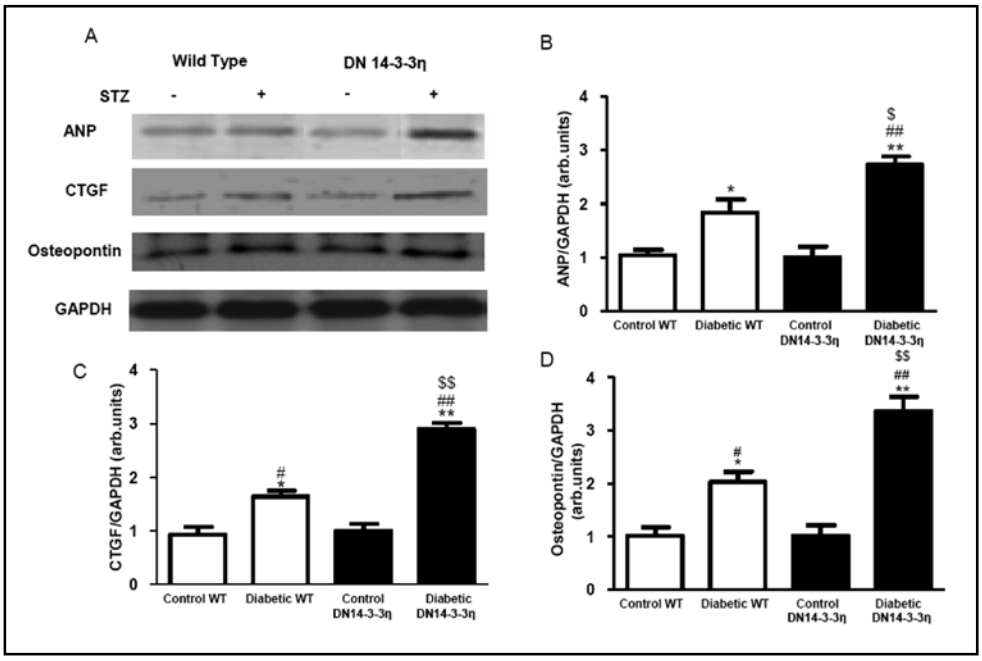

Fig. 4. Left ventricular ANP, CTGF, and osteopontin expression in control and diabetic mice. (A-D) Representative western immunoblots and densitometry analysis using Scion image software for ANP (A and B), CTGF (A and C), and osteopontin (A and D) normalized against GAPDH. White and black bars represent WT and DN 14-3-3η mice respectively. Each bar represents means ± S.E. (n=4 to 5). *P < 0.05 vs. control WT mice; **P < 0.01 vs. control WT mice; $^{\#}P$ < 0.05 vs. control DN 14-3-3η mice; $^{\#\#}P$ < 0.01 vs. control DN 14-3-3η mice; $^{\$}P$ < 0.05 vs. diabetic WT mice on the same day; $^{\$\$}P$ < 0.01 vs. diabetic WT mice on the same day.

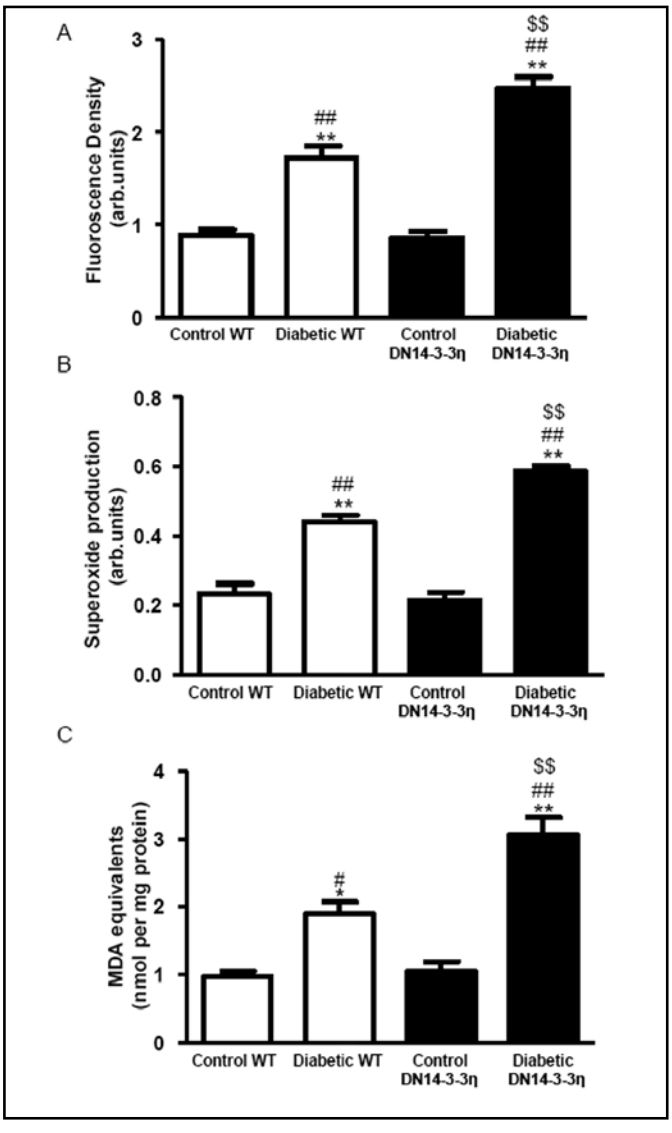

Fig. 5. STZ injection elevates the myocardial ROS and oxidative stress. (A) Intracellular total heart ROS content measured by DCFH assay. (B) Superoxide production from LV homogenates of control and diabetic animals. (C) Bar graph shows MDA levels in control and diabetic mice. White and black bars represent WT and DN 14-3-3η mice respectively. Each bar represents means ± S.E. (n=4 to 5). *P < 0.05 vs. control WT mice; **P < 0.01 vs. control WT mice; $^{\#}P$ < 0.05 vs. control DN 14-3-3η mice; $^{\#\#}P$ < 0.01 vs. control DN 14-3-3η mice; $^{\$\$}P$ < 0.01 vs. diabetic WT mice on the same day.

their normal controls (Fig. 2A-C). Interestingly, NF-κB activation and IκBα degradation were significantly higher in diabetic DN 14-3-3η mice compared to diabetic WT mice.

Cardiac hypertrophy, interstitial fibrosis and related protein expression

The average cross-sectional diameter of cardiac myocyte was slightly increased in WT mice but significantly increased in DN 14-3-3η mice at 28 days after STZ injection when compared to control WT mice and control DN 14-3-3η mice (Fig. 3A-D and M). Myocardial fibrosis was concurrently elevated in both WT and DN 14-3-3η mice at 28 days after STZ injection compared with control WT mice and control DN 14-3-3η mice (Fig. 3E-H and N). In addition,

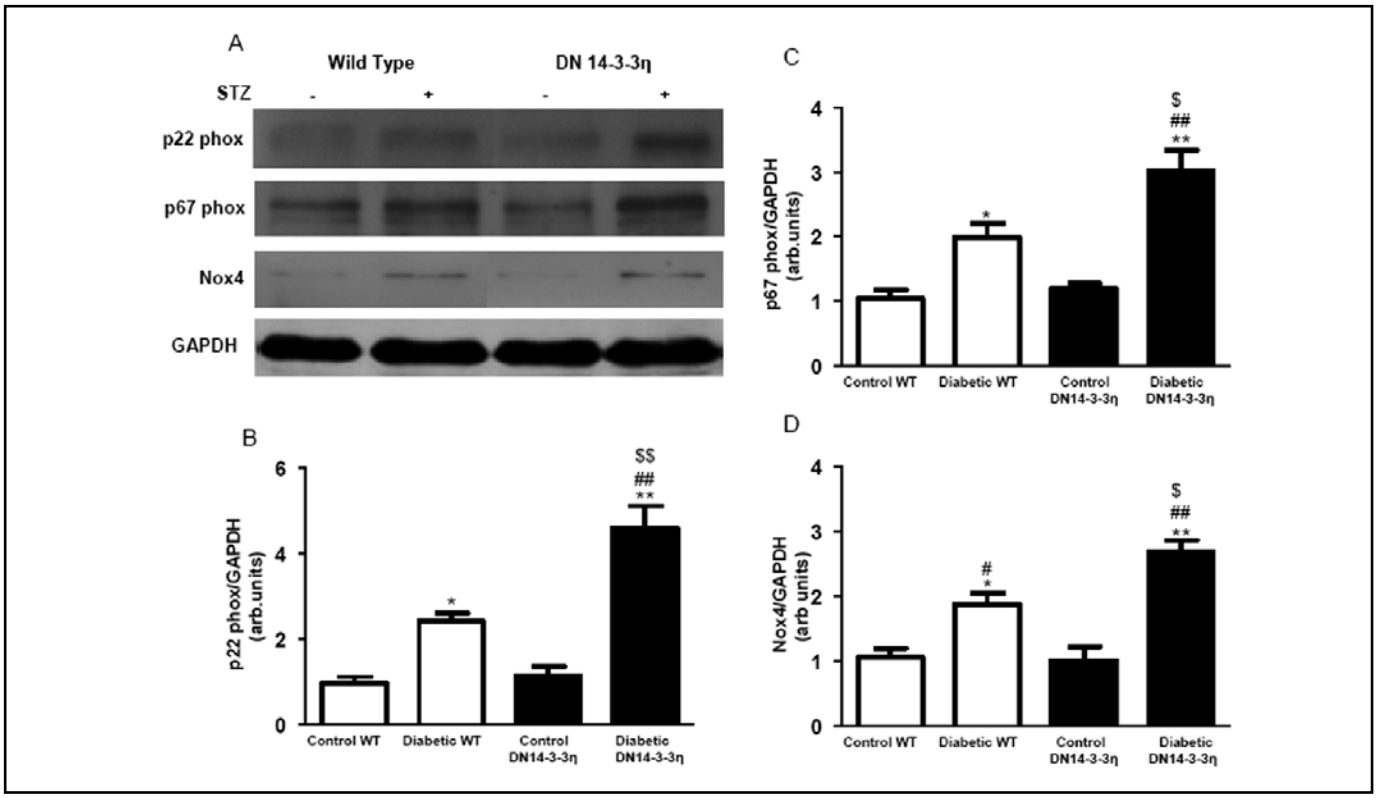

Fig. 6. (A-D) Representative western immunoblots and densitometry analysis using Scion image software for p22 phox, p67 phox, and Nox 4 in control and diabetic mice; Blots were normalized against GAPDH. White and black bars represent WT and DN 14-3-3η mice, respectively. Each bar represents means ± S.E. (n=4 to 5). *$P < 0.05$ vs. control WT mice; **$P < 0.01$ vs. control WT mice; $^{\#}P < 0.05$ vs. control DN 14-3-3η mice; $^{\#\#}P < 0.01$ vs. control DN 14-3-3η mice; $^{\$}P < 0.05$, $^{\$\$}P < 0.01$ vs. diabetic WT mice on the same day.

myocardial fibrosis was also significantly increased in diabetic DN 14-3-3η mice compared with diabetic WT mice (Fig. 3F, H and N). The expression of molecular markers of cardiac hypertrophy such as ANP and pro-fibrotic proteins CTGF and osteopontin expressions were also elevated in WT and DN 14-3-3η mice at 28 days after STZ injection (Fig. 4A-D). Moreover, the elevation was significantly higher in diabetic DN 14-3-3η mice relative to diabetic WT mice (Fig. 4A-D).

Increased ROS

Figure 3I-L shows the intracellular red fluorescence because of the intercalation of ethidium into DNA in the hearts of WT and DN 14-3-3η mice after diabetes induction compared to its respective genetic controls. Diabetes-induced enhancement in ethidium fluorescence was significantly higher in DN 14-3-3η mice compared to WT mice (Fig. 3J and L), indicating an overall increased oxidative stress. Total heart ROS content assessed by DCFH assay was significantly increased in the hearts of WT and DN 14-3-3η mice after diabetes induction compared to its respective genetic controls. However, the level of ROS was significantly higher in diabetic DN 14-3-3η mice (Fig. 5A). In addition, NADPH-dependent O_2^- production by LV homogenates assessed by the cytochrome c reduction was significantly increased in the hearts of diabetic WT and DN 14-3-3η mice compared to its respective genetic controls (Fig. 5B). Interestingly, the ROS production was significantly increased in the hearts of diabetic DN 14-3-3η mice compared to diabetic WT mice (Fig. 5B).

Increased oxidative stress

Thiobarbituric acid-reactive substance was significantly increased in the WT and DN 14-3-3η diabetic heart compared to the control animals (Fig. 5C). However the increase in thiobarbituric acid-reactive substance was higher in diabetic DN 14-3-3η compared to WT mice (Fig. 5C). Myocardial expression of p22 phox, p67 phox and Nox4 were significantly elevated in both WT mice and DN 14-3-3η mice, at 28 days

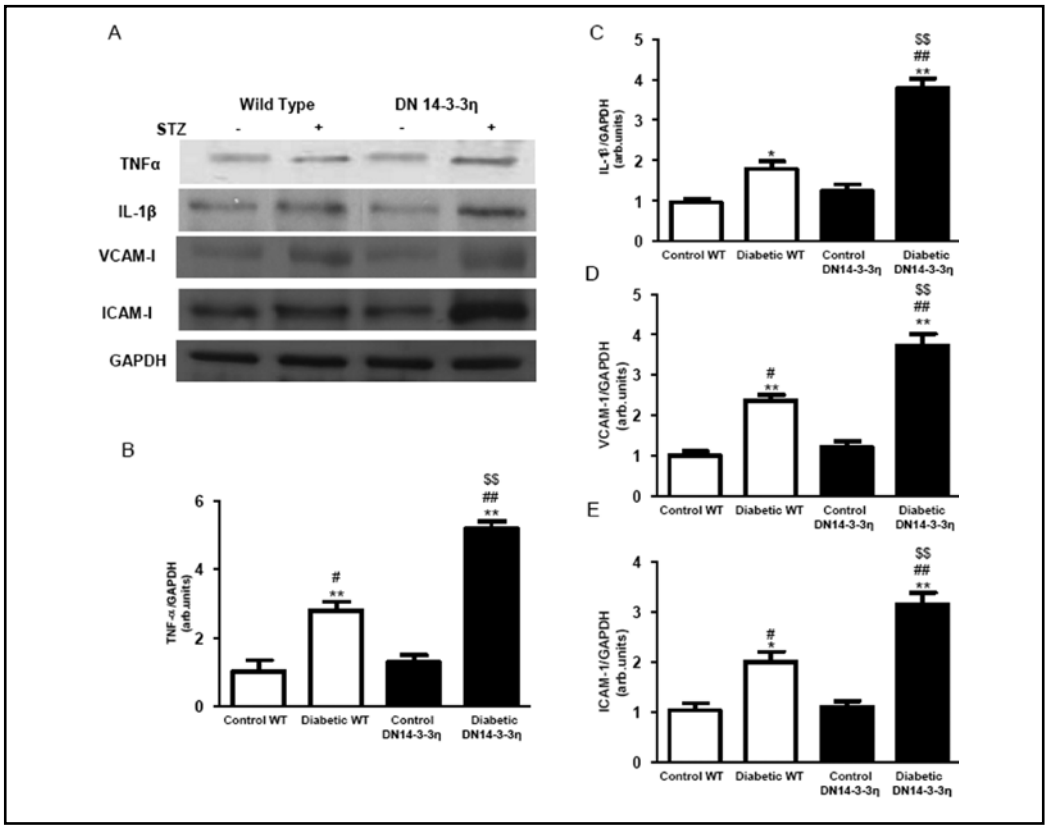

Fig. 7. Left ventricular TNFα, IL-1β, VCAM-I and ICAM-I expression in control and diabetic mice. (A-E) Representative western immunoblots and densitometry analysis using Scion image software for TNFα (A and B), IL-1β, (A and C), VCAM-I (A and D) and ICAM-I (A and E) normalized against GAPDH. White and black bars represent WT and DN 14-3-3η mice respectively. Each bar represents means ± S.E. (n=4 to 5). $*P < 0.05$ vs. control WT mice; $**P < 0.01$ vs. control WT mice; $^{\#}P < 0.05$ vs. control DN 14-3-3η mice; $^{\#\#}P < 0.01$ vs. control DN 14-3-3η mice; $^{\$\$}P < 0.01$ vs. diabetic WT mice on the same day.

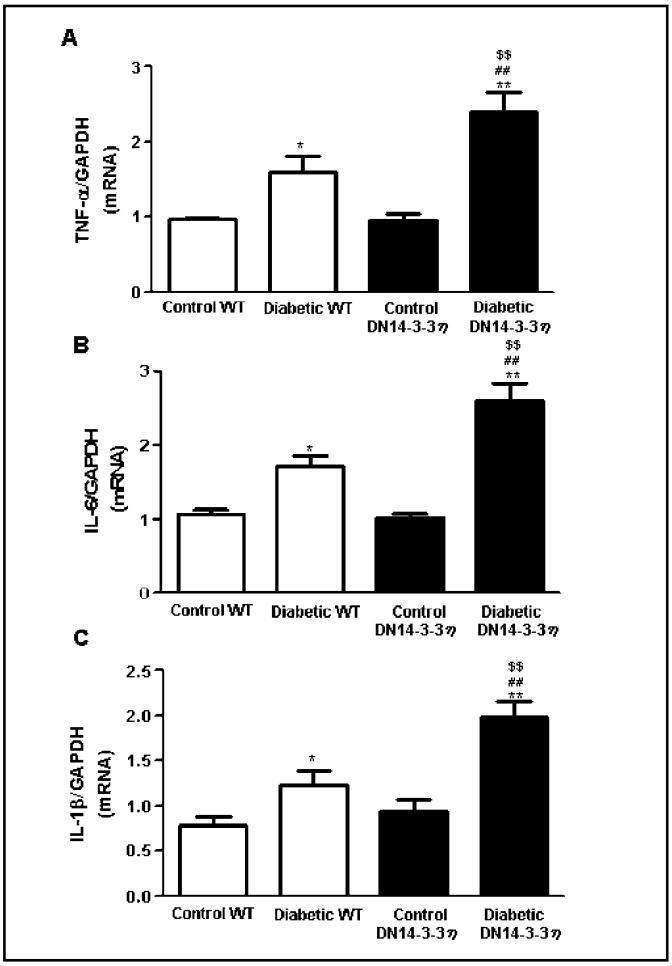

Fig. 8. Left ventricular mRNA expression of TNFα, IL-6 and IL-1β in control and diabetic mice. (A-C) TNFα (A), IL-6 (B) and IL-1β (C) normalized against GAPDH. White and black bars represent WT and DN 14-3-3η mice respectively. Each bar represents means ± S.E. (n=4 to 5). $*P < 0.05$ vs. control WT mice; $**P < 0.01$ vs. control WT mice; $^{\#\#}P < 0.01$ vs. control DN 14-3-3η mice; $^{\$\$}P < 0.01$ vs. diabetic WT mice on the same day.

after STZ injection compared to its respective genetic controls (Fig. 6A-D). Interestingly, the increases in NADPH subunits were significantly higher in diabetic DN 14-3-3η mice than diabetic WT mice.

Increased inflammatory cytokines and cellular adhesion molecules

Cardiac protein levels of pro-inflammatory cytokines, such as TNF-α and IL-1β were significantly increased in both WT and DN 14-3-3η mice at 28 days after diabetes induction. However, the increase was significantly higher in diabetic DN 14-3-3η mice than diabetic WT mice (Fig. 7A-C). Furthermore the protein levels of cellular adhesion molecules ICAM-1 and

VCAM-1 were significantly increased in both WT and DN 14-3-3η mice after diabetes induction and the increase was significantly higher in diabetic DN 14-3-3η mice (Fig.7A, D and E).

mRNA expression of inflammatory cytokines

Cardiac mRNA expression levels of pro-inflammatory cytokines, such as TNF-α, IL-6 and IL-1β were significantly increased in both WT and DN 14-3-3η mice at 28 days after diabetes induction. However, the increases were significantly higher in diabetic DN 14-3-3η mice than diabetic WT mice (Fig. 8A-C).

Discussion

14-3-3 protein belongs to a class of highly conserved proteins involved in regulating apoptosis, adhesion, cellular proliferation, differentiation, survival, and signal transduction pathways [11, 26]. Recently, we have reported that development of diabetic cardiomyopathy is accelerated after disruption of 14-3-3 protein function, in part through enhancement of the Ask-1 signaling pathway [14]. Though, we have implicated the role of 14-3-3 protein, the specific role of 14-3-3 protein in oxidative stress, cardiac inflammation and its downstream signaling after diabetes induction is not known. Our study results indicate that cardiac specific over expression of DN 14-3-3 significantly exacerbated cardiac inflammation characterized by increased cardiac proinflammatory cytokine levels, oxidative stress, fibrosis, hypertrophy and up regulating the LV p38 MAPK, MAPKAPK-2 and NF-κB activation associated with diabetic cardiomyopathy. These results indicate that 14-3-3 protein plays an important role in the mediation of cardiac oxidative stress, inflammation and remodeling processes by regulating p38 MAPK, MAPKAPK-2 and NF-κB signaling pathways associated with diabetic cardiomyopathy.

Overexpression of 14-3-3 protein has been shown to block Ask1-induced apoptosis in HeLa cells [27] and disruption of the Ask1/14-3-3 protein interaction by oxidative stress such as H_2O_2 dramatically enhances apoptosis in COS7 cells [28]. We have previously shown that DN 14-3-3η represents 50% of pan-14-3-3 protein in the LV of DN 14-3-3η mice [15]. In our previous study, we observed significant enhancement of Ask1 activity in diabetic DN 14-3-3η mice [14] and Ask1 activation followed by that of p38 MAPK is reported to enhance myocardial monocyte chemoattractant protein 1 expression in cardiac fibroblasts [29]. Cardiac phosphorylation of p38 MAPK was significantly reduced by atorvastatin in STZ-induced diabetic animals and improves cardiac function [30] and reorganization of actin cytoskeleton induced during cellular stresses is mediated via the p38 MAPKAPK-2–HSP27 pathway [31, 32]. In this study, we found enhanced activation of p38 MAPK and its downstream effector, p38 MAPKAPK-2 in diabetic DN 14-3-3 mice relative to diabetic WT mice. Hence, we propose that diabetes-induced Ask1 signaling activates its downstream effectors p38 MAPK and MAPAKAPK-2 and these findings suggest that endogenous cardiac resident 14-3-3 protein plays a crucial role in limiting Ask1-p38 MAPK and MAPKAPK-2 signaling pathways in the diabetic myocardium.

It has been demonstrated that of Ask1 is involved G-protein coupled receptor agonist-induced cardiac hypertrophy mediated through NF-κB activation [33] and we believe that it likely contributes to chronic tissue damage in diabetic heart disease. NF-κB is known to be activated by p38 MAPK in cardiomyocytes [33]. Recently, we have clearly indicated that p38 MAPK and its downstream effector MAPKAPK-2 play a significant role in the development of LV cardiomyocyte hypertrophy and fibrosis after experimental diabetes [34] and in the present study, we found increased MAPK and NF-κB activation in LV of diabetic DN 14-3-3η mice with significant myocyte enlargement and fibrosis. Moreover, Ask1-/- mice were reported to be resistant to angiotensin II (Ang II)-induced hypertrophy [35], and we have also observed marked elevation in Ang II levels [21] with significant hypertrophy and fibrosis in DN 14-3-3η mice after induction of diabetes [20, 21]. It is therefore possible that 14-3-3 protein regulates cardiac hypertrophy associated with diabetes may also be mediated by the Ang II-Ask1-MAPK-NF-κB axis.

Accumulating evidence show that ROS play a key role in the initiation and progression of cardiovascular diseases [34, 36, 37] and high glucose can induce the activation of p22 phox, a component of the NADPH oxidase, via de nova synthesis of diacyl glycerol [38]. Recently, we have reported that p38 MAPK is associated with the onset of apoptosis, increased NADPH oxidase subunits expression, ROS production and cardiac remodeling in diabetic mouse hearts [34]. Very importantly, NADPH oxidase–mediated ROS are mandatory for the development of aldosterone-induced cardiac inflammation and fibrosis [39]. Ask-1 deficiency, an upstream target of MAPK significantly inhibited aldosterone-induced

NADPH oxidase activation and superoxide generation, indicating the contribution of Ask-1 to aldosterone-induced cardiac NADPH oxidase activation [40]. Recently, we have reported that 14-3-3 protein aids the oxidoreductase system in regulating oxidative stress after diabetes induction and mechanism remains to be defined [14]. In this work, we found that DN 14-3-3 significantly exacerbated diabetes-induced ROS generation, indicating the contribution of 14-3-3 protein and p38 MAPK to diabetes-induced cardiac ROS production. To further elucidate the underlying molecular mechanism, we examined the effect of MAPK activation on NADPH oxidase subunits and found that MAPK activation significantly exacerbated diabetes-induced cardiac NADPH oxidase subunits in diabetic DN 14-3-3 mice. However, the principle behind the role of 14-3-3 protein in diabetes-induced NADPH oxidase activation needs further clarification. These findings suggest that endogenous cardiac resident 14-3-3 protein plays a crucial role in limiting p38 MAPK mediated cardiac oxidative stress in the diabetic myocardium.

NF-κB might participate in some of the downstream effects of NADPH oxidase on cardiac hypertrophy and also regulates the expression of inflammatory genes, including TNF-α and IL-6 [41-43]. Diabetic cardiomyopathy is associated with increased levels of the pro-inflammatory cytokines TNF-α and IL1-β [7] and pharmacological inhibition of p38 MAPK significantly attenuated the expression of cardiac inflammatory markers such as TNF-α, IL-1β and IL-6, and collagen content associated with diabetic cardiomyopathy [44]. Cardiac inflammation is accompanied by increased expression of the ICAM-1 and VCAM-1[45] and linked with decreased LV function, not only in diabetic cardiomyopathy, but also for example in myocardial infarction, pressure overload, and dilated cardiomyopathy [46-48]. Moreover, we have found in this and previous studies, that, increased cytokines are one of the mechanisms leading to LV dysfunction in diabetes mellitus, as demonstrated by reduced LV fractional shortening, increased TNF-α, IL-1β and cellular adhesion molecules in diabetic DN 14-3-3 mice relative to diabetic WT mice. These results clearly indicate that 14-3-3 protein plays a significant role in MAPK-NF-κB mediated cardiac dysfunction and production of LV inflammatory cytokines after experimental diabetes.

In conclusion, our results strongly indicate that development of diabetic cardiomyopathy is accelerated after disruption of 14-3-3 protein function, in part through enhancement of the MAPK-NF-κB signaling pathway. This process subsequently contributes to increased oxidative stress and myocardial remodeling events such as inflammation, hypertrophy and interstitial fibrosis and aids the transition of compensated diabetic hearts to de-compensated failing hearts.

Acknowledgements

This research was supported by grants from Yujin Memorial Grant; the Ministry of Education, Culture, Sports, Science and Technology of Japan; Promotion and Mutual Aid Corporation for Private Schools of Japan and grants from Niigata prefecture.

References

1 Spector KS: Diabetic cardiomyopathy. Clin Cardiol 1998;21:885-887.

2 Poornima IG, Parikh P, Shannon RP: Diabetic cardiomyopathy: The search for a unifying hypothesis. Circ Res 2006;98:596-605.

3 Bell DS: Diabetic cardiomyopathy. Diabetes Care 2003;26:2949-2951.

4 Tschope C, Walther T, Koniger J, Spillmann F, Westermann D, Escher F, Pauschinger M, Pesquero JB, Bader M, Schultheiss HP, Noutsias M: Prevention of cardiac fibrosis and left ventricular dysfunction in diabetic cardiomyopathy in rats by transgenic expression of the human tissue kallikrein gene. FASEB J 2004;18:828-835.

5 Asbun J, Villarreal FJ: The pathogenesis of myocardial fibrosis in the setting of diabetic cardiomyopathy. J Am Coll Cardiol 2006;47:693-700.

6 Tschope C, Spillmann F, Rehfeld U, Koch M, Westermann D, Altmann C, Dendorfer A, Walther T, Bader M, Paul M, Schultheiss HP, Vetter R: Improvement of defective sarcoplasmic reticulum Ca^{2+} transport in diabetic heart of transgenic rats expressing the human kallikrein-1 gene. FASEB J 2004;18:1967-1969.

7 Tschope C, Walther T, Escher F, Spillmann F, Du J, Altmann C, Schimke I, Bader M, Sanchez-Ferrer CF, Schultheiss HP, Noutsias M: Transgenic activation of the kallikrein-kinin system inhibits intramyocardial inflammation, endothelial dysfunction and oxidative stress in experimental diabetic cardiomyopathy. FASEB J 2005;19:2057-2059.

8 Azar ST, Salti I, Zantout MS, Major S: Alterations in plasma transforming growth factor beta in normoalbuminuric type 1 and type 2 diabetic patients. J Clin Endocrinol Metab 2000;85:4680-4682.

9 Barnes PJ, Karin M: Nuclear factor-kappab: A pivotal transcription factor in chronic inflammatory diseases. N Engl J Med 1997;336:1066-1071.
10 Torre-Amione G, Sestier F, Radovancevic B, Young J: Broad modulation of tissue responses (immune activation) by celacade may favorably influence pathologic processes associated with heart failure progression. Am J Cardiol 2005;95:30C-37C; discussion 38C-40C.
11 Wilker E, Yaffe MB: 14-3-3 proteins-a focus on cancer and human disease. J Mol Cell Cardiol 2004;37:633-642.
12 Tobiume K, Matsuzawa A, Takahashi T, Nishitoh H, Morita K, Takeda K, Minowa O, Miyazono K, Noda T, Ichijo H: Ask1 is required for sustained activations of JNK/p38 MAP kinases and apoptosis. EMBO Rep 2001;2:222-228.
13 Takeda K, Hatai T, Hamazaki TS, Nishitoh H, Saitoh M, Ichijo H: Apoptosis signal-regulating kinase 1 (ASK1) induces neuronal differentiation and survival of pc12 cells. J Biol Chem 2000;275:9805-9813.
14 Thandavarayan RA, Watanabe K, Ma M, Veeraveedu PT, Gurusamy N, Palaniyandi SS, Zhang S, Muslin AJ, Kodama M, Aizawa Y: 14-3-3 protein regulates ASK1 signaling and protects against diabetic cardiomyopathy. Biochem Pharmacol 2008;75:1797-1806.
15 Xing H, Zhang S, Weinheimer C, Kovacs A, Muslin AJ: 14-3-3 proteins block apoptosis and differentially regulate MAPK cascades. EMBO J 2000;19:349-358.
16 Gurusamy N, Watanabe K, Ma M, Zhang S, Muslin AJ, Kodama M, Aizawa Y: Dominant negative 14-3-3 promotes cardiomyocyte apoptosis in early stage of type I diabetes mellitus through activation of JNK. Biochem Biophys Res Commun 2004;320:773-780.
17 Kuhad A, Chopra K: Attenuation of diabetic nephropathy by tocotrienol: Involvement of NFκB signaling pathway. Life Sci 2009;84:296-301.
18 Li JM, Gall NP, Grieve DJ, Chen M, Shah AM: Activation of NADPH oxidase during progression of cardiac hypertrophy to failure. Hypertension 2002;40:477-484.
19 Yan LJ, Rajasekaran NS, Sathyanarayanan S, Benjamin IJ: Mouse HSF1 disruption perturbs redox state and increases mitochondrial oxidative stress in kidney. Antioxid Redox Signal 2005;7:465-471.
20 Gurusamy N, Watanabe K, Ma M, Zhang S, Muslin AJ, Kodama M, Aizawa Y: Inactivation of 14-3-3 protein exacerbates cardiac hypertrophy and fibrosis through enhanced expression of protein kinase C beta 2 in experimental diabetes. Biol Pharm Bull 2005;28:957-962.
21 Gurusamy N, Watanabe K, Ma M, Prakash P, Hirabayashi K, Zhang S, Muslin AJ, Kodama M, Aizawa Y: Glycogen synthase kinase 3beta together with 14-3-3 protein regulates diabetic cardiomyopathy: Effect of losartan and tempol. FEBS Lett 2006;580:1932-1940.
22 Miller FJ Jr, Gutterman DD, Rios CD, Heistad DD, Davidson BL: Superoxide production in vascular smooth muscle contributes to oxidative stress and impaired relaxation in atherosclerosis. Circ Res 1998;82:1298-1305.
23 Takaya T, Kawashima S, Shinohara M, Yamashita T, Toh R, Sasaki N, Inoue N, Hirata K, Yokoyama M: Angiotensin ii type 1 receptor blocker telmisartan suppresses superoxide production and reduces atherosclerotic lesion formation in apolipoprotein E-deficient mice. Atherosclerosis 2006;186:402-410.
24 Neilan TG, Blake SL, Ichinose F, Raher MJ, Buys ES, Jassal DS, Furutani E, Perez-Sanz TM, Graveline A, Janssens SP, Picard MH, Scherrer-Crosbie M, Bloch KD: Disruption of nitric oxide synthase 3 protects against the cardiac injury, dysfunction, and mortality induced by doxorubicin. Circulation 2007;116:506-514.
25 Thandavarayan RA, Watanabe K, Sari FR, Ma M, Lakshmanan AP, Giridharan VV, Gurusamy N, Nishida H, Konishi T, Zhang S, Muslin AJ, Kodama M, Aizawa Y: Modulation of doxorubicin-induced cardiac dysfunction in dominant-negative p38alpha mitogen-activated protein kinase mice. Free Radic Biol Med 2010;49:1422-1431.
26 Zarich SW, Nesto RW: Diabetic cardiomyopathy. Am Heart J 1989;118:1000-1012.
27 Zhang L, Chen J, Fu H: Suppression of apoptosis signal-regulating kinase 1-induced cell death by 14-3-3 proteins. Proc Natl Acad Sci U S A 1999;96:8511-8515.
28 Goldman EH, Chen L, Fu H: Activation of apoptosis signal-regulating kinase 1 by reactive oxygen species through dephosphorylation at serine 967 and 14-3-3 dissociation. J Biol Chem 2004;279:10442-10449.
29 Omura T, Yoshiyama M, Kim S, Matsumoto R, Nakamura Y, Izumi Y, Ichijo H, Sudo T, Akioka K, Iwao H, Takeuchi K, Yoshikawa J: Involvement of apoptosis signal-regulating kinase-1 on angiotensin II-induced monocyte chemoattractant protein-1 expression. Arterioscler Thromb Vasc Biol 2004;24:270-275.
30 Van Linthout S, Riad A, Dhayat N, Spillmann F, Du J, Dhayat S, Westermann D, Hilfiker-Kleiner D, Noutsias M, Laufs U, Schultheiss HP, Tschope C: Anti-inflammatory effects of atorvastatin improve left ventricular function in experimental diabetic cardiomyopathy. Diabetologia 2007;50:1977-1986.
31 Guay J, Lambert H, Gingras-Breton G, Lavoie JN, Huot J, Landry J: Regulation of actin filament dynamics by p38 map kinase-mediated phosphorylation of heat shock protein 27. J Cell Sci 1997;110:357-368.
32 Huot J, Houle F, Marceau F, Landry J: Oxidative stress-induced actin reorganization mediated by the p38 mitogen-activated protein kinase/heat shock protein 27 pathway in vascular endothelial cells. Circ Res 1997;80:383-392.
33 Hirotani S, Otsu K, Nishida K, Higuchi Y, Morita T, Nakayama H, Yamaguchi O, Mano T, Matsumura Y, Ueno H, Tada M, Hori M: Involvement of nuclear factor-kappaB and apoptosis signal-regulating kinase 1 in G-protein-coupled receptor agonist-induced cardiomyocyte hypertrophy. Circulation 2002;105:509-515.
34 Thandavarayan RA, Watanabe K, Ma M, Gurusamy N, Veeraveedu PT, Konishi T, Zhang S, Muslin AJ, Kodama M, Aizawa Y: Dominant-negative p38alpha mitogen-activated protein kinase prevents cardiac apoptosis and remodeling after streptozotocin-induced diabetes mellitus. Am J Physiol Heart Circ Physiol 2009;297:H911-919.
35 Izumiya Y, Kim S, Izumi Y, Yoshida K, Yoshiyama M, Matsuzawa A, Ichijo H, Iwao H: Apoptosis signal-regulating kinase 1 plays a pivotal role in angiotensin II-induced cardiac hypertrophy and remodeling. Circ Res 2003;93:874-883.
36 Griendling KK, Sorescu D, Ushio-Fukai M: NAD(P)H oxidase: Role in cardiovascular biology and disease. Circ Res 2000;86:494-501.
37 Takimoto E, Kass DA: Role of oxidative stress in cardiac hypertrophy and remodeling. Hypertension 2007;49:241-248.
38 Inoguchi T, Li P, Umeda F, Yu HY, Kakimoto M, Imamura M, Aoki T, Etoh T, Hashimoto T, Naruse M, Sano H, Utsumi H, Nawata H: High glucose level and free fatty acid stimulate reactive oxygen species production through protein kinase c-dependent activation of NAD(P)H oxidase in cultured vascular cells. Diabetes 2000;49:1939-1945.

39 Johar S, Cave AC, Narayanapanicker A, Grieve DJ, Shah AM: Aldosterone mediates angiotensin II-induced interstitial cardiac fibrosis via a nox2-containing NADPH oxidase. FASEB J 2006;20:1546-1548.
40 Nakamura T, Kataoka K, Fukuda M, Nako H, Tokutomi Y, Dong YF, Ichijo H, Ogawa H, Kim-Mitsuyama S: Critical role of apoptosis signal-regulating kinase 1 in aldosterone/salt-induced cardiac inflammation and fibrosis. Hypertension 2009;54:544-551.
41 Liu SF, Malik AB: Nf-kappa B activation as a pathological mechanism of septic shock and inflammation. Am J Physiol Lung Cell Mol Physiol 2006;290:L622-L645.
42 Liu SF, Ye X, Malik AB: Inhibition of NF-kappaB activation by pyrrolidine dithiocarbamate prevents in vivo expression of proinflammatory genes. Circulation 1999;100:1330-1337.
43 Satoh M, Ogita H, Takeshita K, Mukai Y, Kwiatkowski DJ, Liao JK: Requirement of RAC1 in the development of cardiac hypertrophy. Proc Natl Acad Sci USA 2006;103:7432-7437.
44 Westermann D, Rutschow S, Van Linthout S, Linderer A, Bucker-Gartner C, Sobirey M, Riad A, Pauschinger M, Schultheiss HP, Tschope C: Inhibition of p38 mitogen-activated protein kinase attenuates left ventricular dysfunction by mediating pro-inflammatory cardiac cytokine levels in a mouse model of diabetes mellitus. Diabetologia 2006;49:2507-2513.
45 Westermann D, Van Linthout S, Dhayat S, Dhayat N, Escher F, Bucker-Gartner C, Spillmann F, Noutsias M, Riad A, Schultheiss HP, Tschope C: Cardioprotective and anti-inflammatory effects of interleukin converting enzyme inhibition in experimental diabetic cardiomyopathy. Diabetes 2007;56:1834-1841.
46 Steenbergen C: The role of p38 mitogen-activated protein kinase in myocardial ischemia/reperfusion injury; relationship to ischemic preconditioning. Basic Res Cardiol 2002;97:276-285.
47 Meldrum DR: Tumor necrosis factor in the heart. Am J Physiol 1998;274:R577-595.
48 Nian M, Lee P, Khaper N, Liu P: Inflammatory cytokines and postmyocardial infarction remodeling. Circ Res 2004;94:1543-1553.